Electronic Supplementary Information

Experimental section

Materials: Ethanol (C_2H_5OH) was provided by Chengdu Haixing Chemical Reagent Factory. Potassium hydroxide (KOH), sodium hydroxide (NaOH), hydrochloric acid (HCl), cobalt chloride hydrate ($CoCl_2·6H_2O$), copper chloride hydrate ($CuCl_2·2H_2O$), and urea ($CO(NH_2)_2$) were bought from Chengdu Kelong Chemical Regent Co. Ltd. Sodium sulfide nonahydrate ($Na_2S·9H_2O$), $RuCl_3·3H_2O$, and a Nafion (5 wt%) solution were bought from Sigma–Aldrich Chemical Reagent Co., Ltd. (Shanghai, China). Copper foam (CF) was purchased from Changsha Liyuan New Material Co., Ltd., and was pretreated in HCl, ethanol and deionized water several times to remove the surface impurities. The water used throughout all experiments was purified through a Millipore system and all the reagents and chemicals were used as received without further purification.

Preparation of $CuCo_2$–hydroxide nanowire array precursor: Firstly, 2 mmol $CuCl_2·2H_2O$, 4 mmol $CoCl_2·6H_2O$ and 12 mmol urea were dissolved in 35 mL ultrapure water under vigorous magnetic stirring for 10 min. Then, the above clear solution was transferred to a 50 mL Teflon–lined stainless steel autoclave and then a piece of pre–cleaned CF (2 cm × 3 cm) was immersed into the solution. Thirdly, the autoclave was sealed and maintained at 120 °C for 6 h in an electric oven. After the autoclave cooled naturally to room temperature, the resulting CF was taken out and washed with distilled water and ethanol several times, followed by drying at 70 °C for 3 h. For comparison, monometallic Cu– and Co–hydroxide precursors and bimetallic CuCo–hydroxide precursors with varied Co/Cu ratios were prepared by adjusting the Co^{2+}/Cu^{2+} salt ratios, ensuring the total mole number of Co^{2+} and Cu^{2+} ions is 6 mmol without any changes made in the urea amount, and the corresponding bimetallic products are denoted as Cu_3Co–, Cu_2Co–, CuCo–, and $CuCo_3$–hydroxide precursor, respectively.

Preparation of hierarchical $CuCo_2S_4$ nanoarray on CF: 0.8 mmol $Na_2S·9H_2O$ was dissolved in 40 mL ultrapure water under vigorous stirring for 5 min and then the

pellucid solution was transferred to a 50 mL Teflon–lined stainless–steel autoclave with a piece of CF with $CuCo_2$–hydroxide precursor. The autoclave was sealed and maintained at 150 °C for 6 h in an electric oven. After cooled down naturally to room temperature, the sample was taken out and washed with distilled water and ethanol several times, followed by drying at 70 °C for 3 h in vacuum. Monometallic copper sulphide on CF (Cu–S/CF) and cobalt sulphide on CF (Co–S/CF) and bimetallic Cu_3Co–, Cu_2Co–, CuCo–, and $CuCo_3$–sulphide on CF (Cu_3Co–S/CF, Cu_2Co–S/CF, CuCo–S/CF, and $CuCo_3$–S/CF, respectively) were prepared in a similar way.

Synthesis of RuO_2: RuO_2 was prepared according to previous publication.[1] In brief, 2.61 g of $RuCl_3 \cdot 3H_2O$ was dissolved in 100 mL ultrapure water and stirred for 10 min at 100 °C. Then 30 mL NaOH solution (1.0 M) was added into the above solution and stirring for 45 min at 100 °C. After that, the mixed solution was centrifuged for 10 min and filtered. The precipitates were collected, and washed with distilled water several times. Finally, the product was dried at 80 °C overnight and then annealed at 350 °C for 1 h in air atmosphere. The as–prepared RuO_2 powder (0.01 g) was dispersed into a solution of Nafion, ethanol and ultrapure water with a volume ratio of 10/250/250 *via* sonication, and deposited onto CF with a loading of 3.6 mg cm^{-2}.

Characterizations: X–ray diffraction (XRD) measurements were operated on a LabX XRD–6100 X–ray diffractometer with Cu Kα radiation (40 kV, 30 mA) at a wavelength 1.54 Å (SHIMADZU, Japan). Scanning electron microscope (SEM) images were recorded on a XL30 ESEM FEG scanning electron microscope with an accelerating voltage of 20 kV. Transmission electron microscopy (TEM) images were collected on a HITACHI H–8100 electron microscopy (Hitachi, Tokyo, Japan) with an accelerating voltage of 200 kV. X–ray photoelectron spectroscopy (XPS) measurements were made on an ESCALABMK II X–ray photoelectron spectrometer using Mg as the excitation source.

Electrochemical measurements: Electrochemical measurements were conducted on a CHI 660E electrochemical analyzer (CH Instruments, Inc., Shanghai) in a standard three–electrode system using a $CuCo_2S_4$/CF as the working electrode. A graphite plate and an Hg/HgO were used as the counter electrode and the reference electrode,

respectively. All potentials reported in this work were calibrated to RHE other than especially explained, using the following equation: E (RHE) = E (Hg/HgO) + (0.098+ 0.0592 pH) V. All such experiments were carried out at room temperature (298.15 K) *via* the adjustment of air condition and heating support, ensuring the variation of diffusion coefficient within 1%.

Turnover frequency (TOF) calculations: To calculate TOF, we need to calculate the surface concentration of active sites associated with the redox Cu and Co species by electrochemistry. The linear relationship between the plot of the oxidation peak current densities for redox Cu and Co species and scan rates can be derived from the electrochemical cyclic voltammetry scans according to the following equation:

$$\text{Slope} = n^2F^2A\Gamma_0/RT$$

Where n representing the number of electrons transferred is 1 assuming a one–electron process for oxidation of Cu and Co centers in $CuCo_2S_4$; F is Faraday's constant (96485 C mol^{-1}); A is the geometrical surface area of the electrode; Γ_0 is the surface concentration of active sites (mol cm^{-2}), and R and T are the ideal gas constant and the absolute temperature, respectively.[2]

TOF values can be finally calculated based on the formula:

$$\text{TOF} = jA/4Fm$$

Where j is the current density, 4 indicates the mole of electrons consumed for one mole of O_2 evolution, and m is the mole number of active sites.[3]

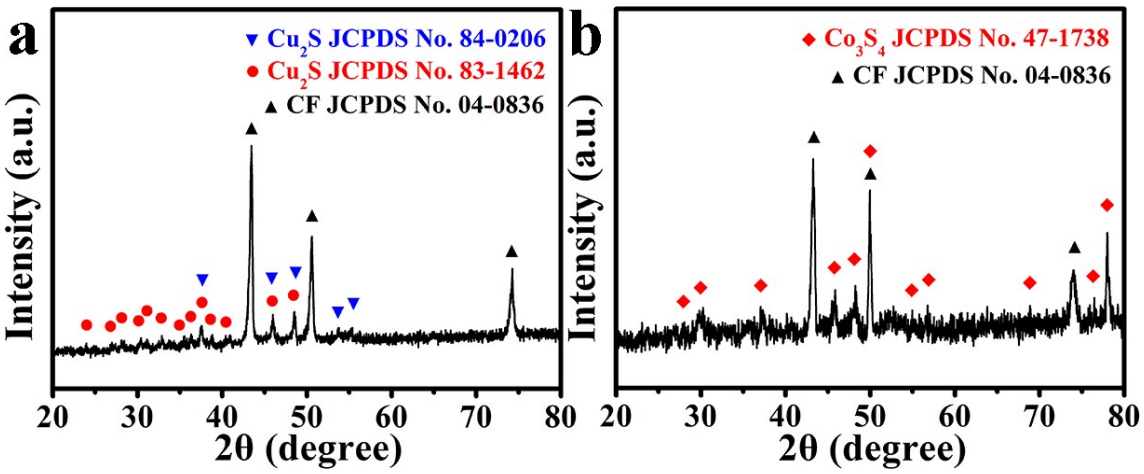

Fig. S1. XRD patterns for (a) Cu–S/CF and (b) Co–S/CF.

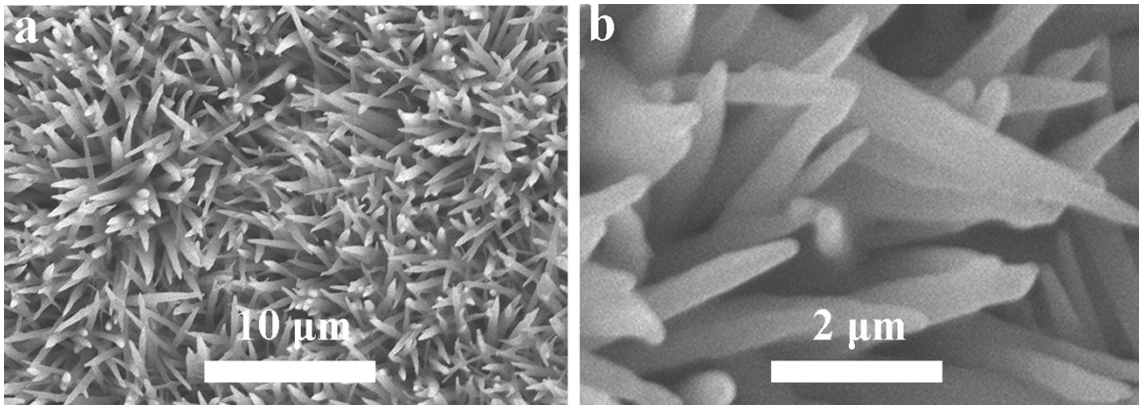

Fig. S2. SEM images for $CuCo_2$–hydroxide precursor on CF.

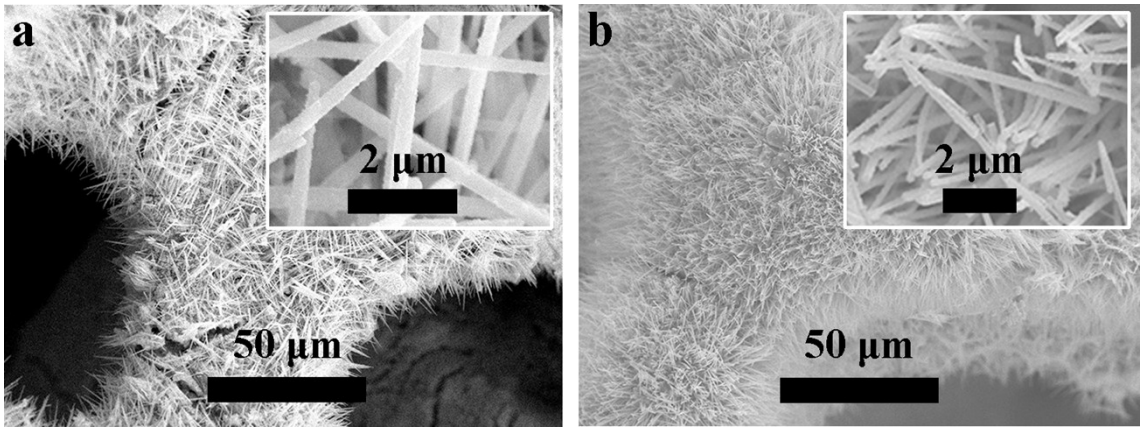

Fig. S3. SEM images for (a) Cu–S/CF and (b) Co–S/CF.

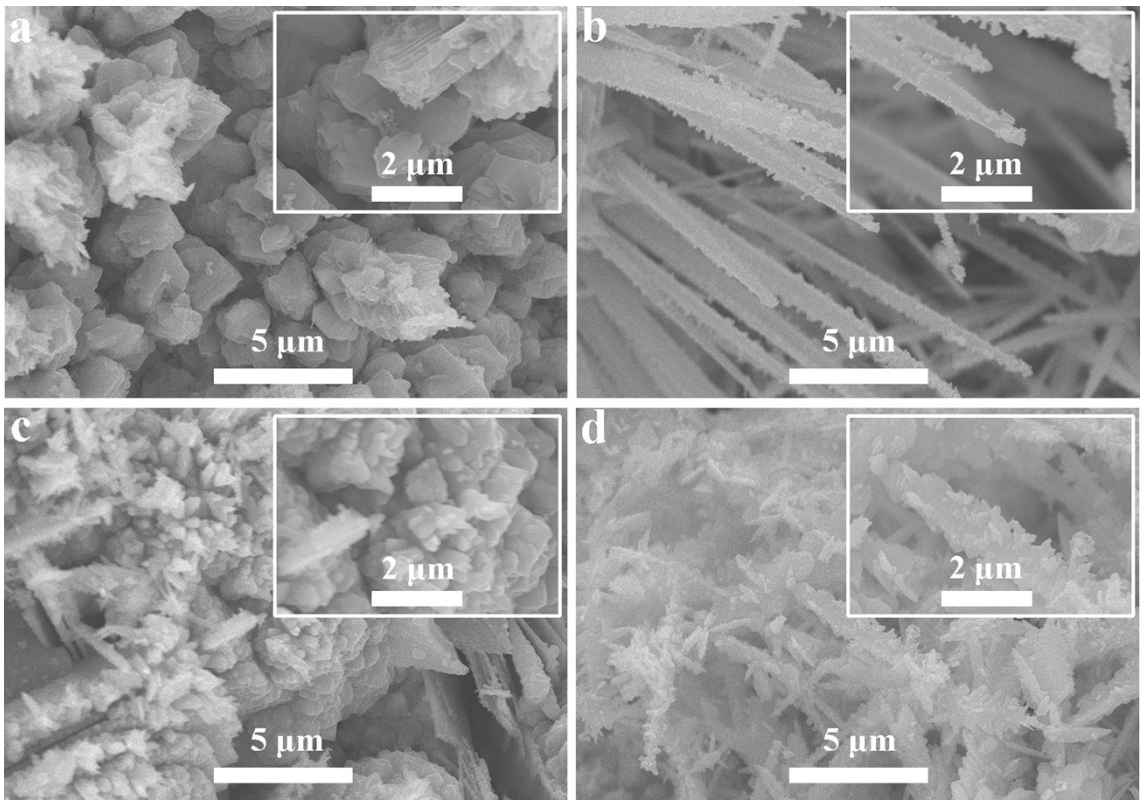

Fig. S4. SEM images for (a) Cu_3Co–S/CF, (b) Cu_2Co–S/CF, (c) CuCo–S/CF, and (d) $CuCo_3$–S/CF.

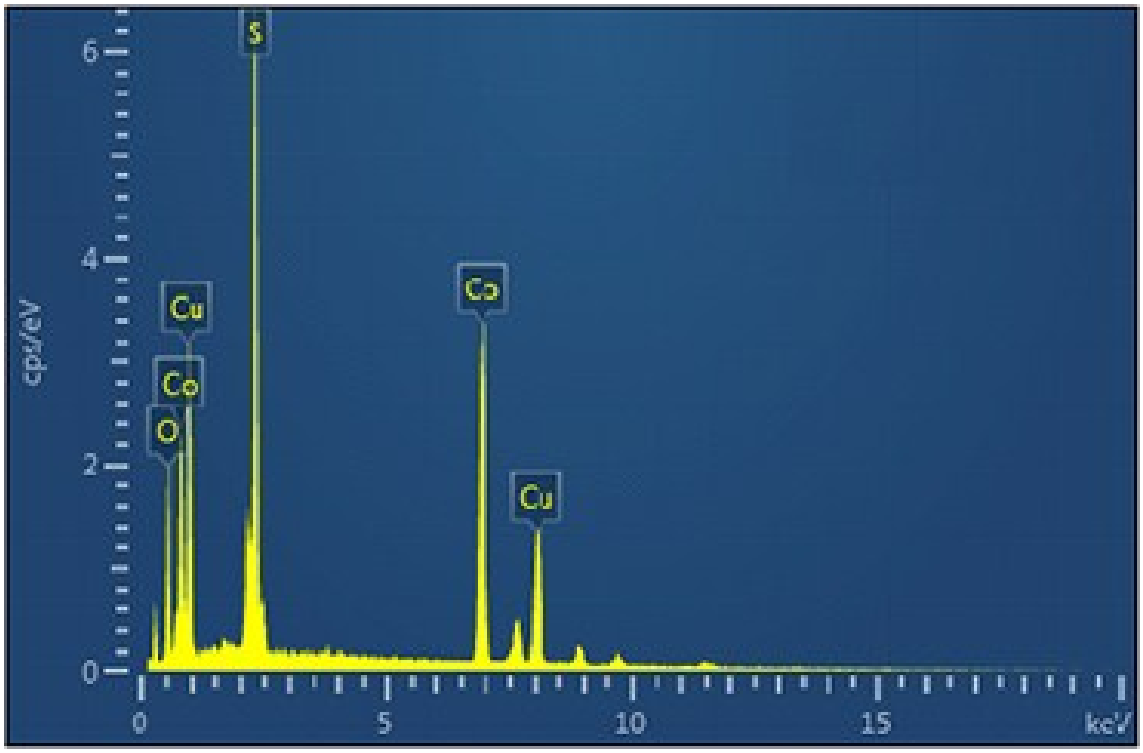

Fig. S5. EDX spectrum for $CuCo_2S_4$/CF.

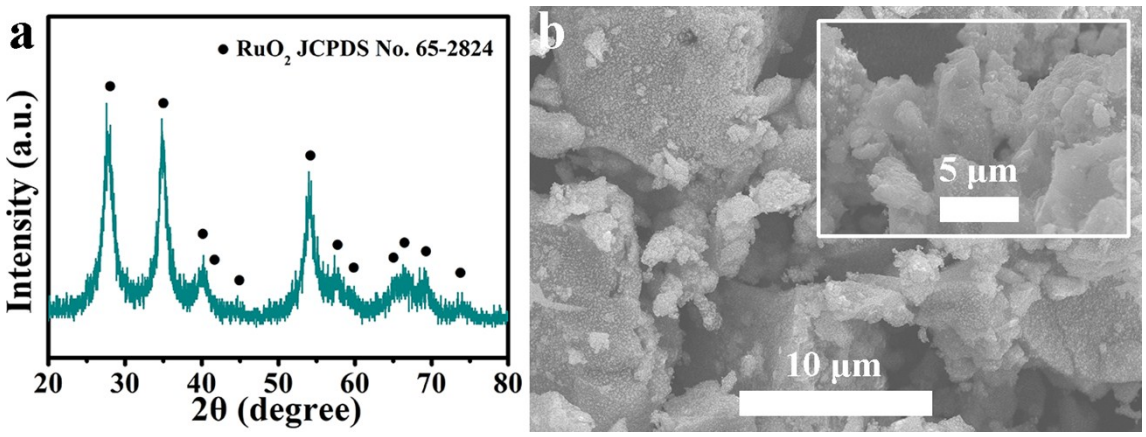

Fig. S6. (a) XRD pattern and (b) SEM images for RuO_2.

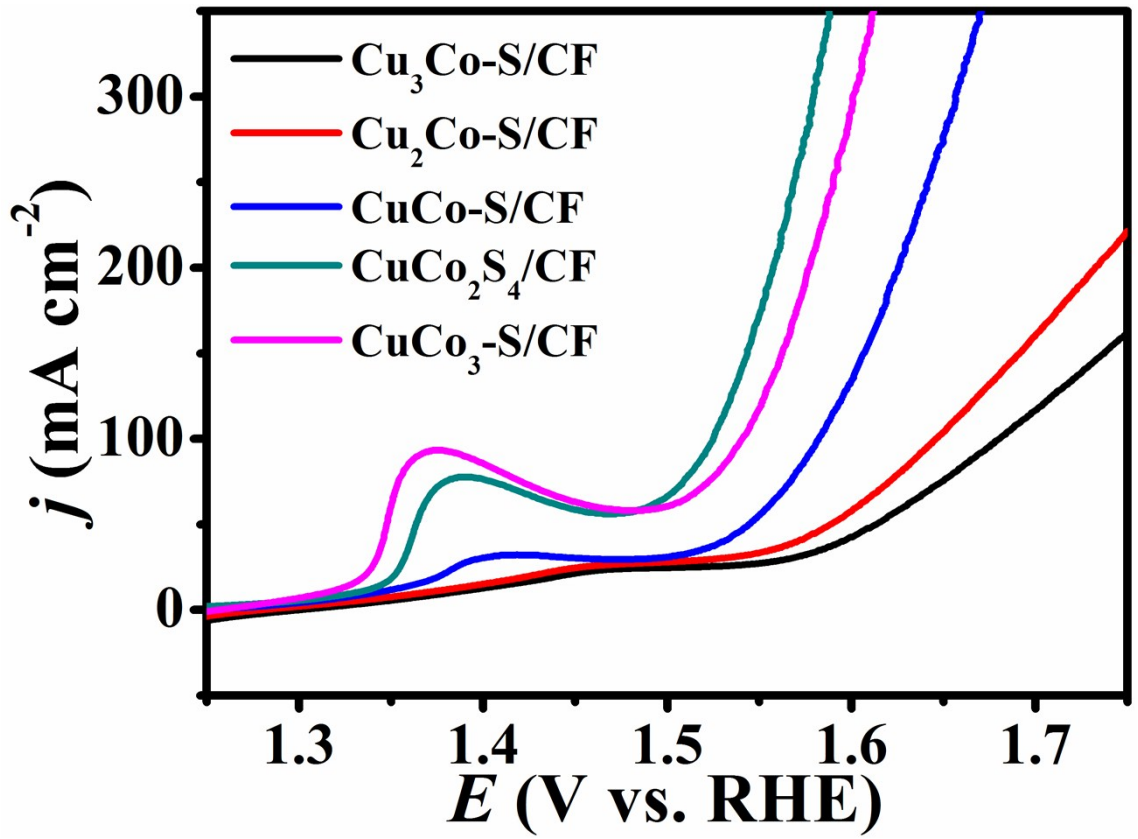

Fig. S7. LSV curves of Cu_3Co–S/CF, Cu_2Co–S/CF, CuCo–S/CF, $CuCo_2S_4$/CF, and $CuCo_3$–S/CF with a scan rate of 5 mV s^{-1} for water oxidation.

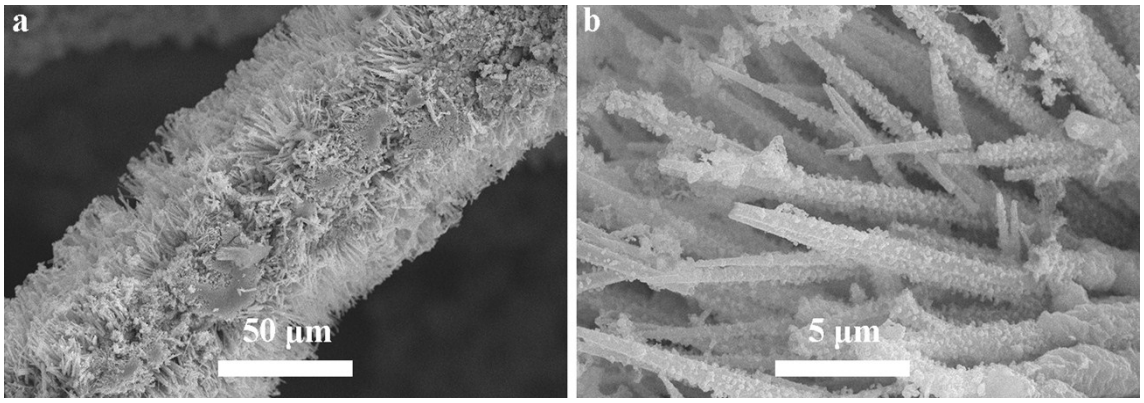

Fig. S8. (a) Low- and (b) magnification SEM images for $CuCo_2S_4$/CF after water oxidation electrolysis.

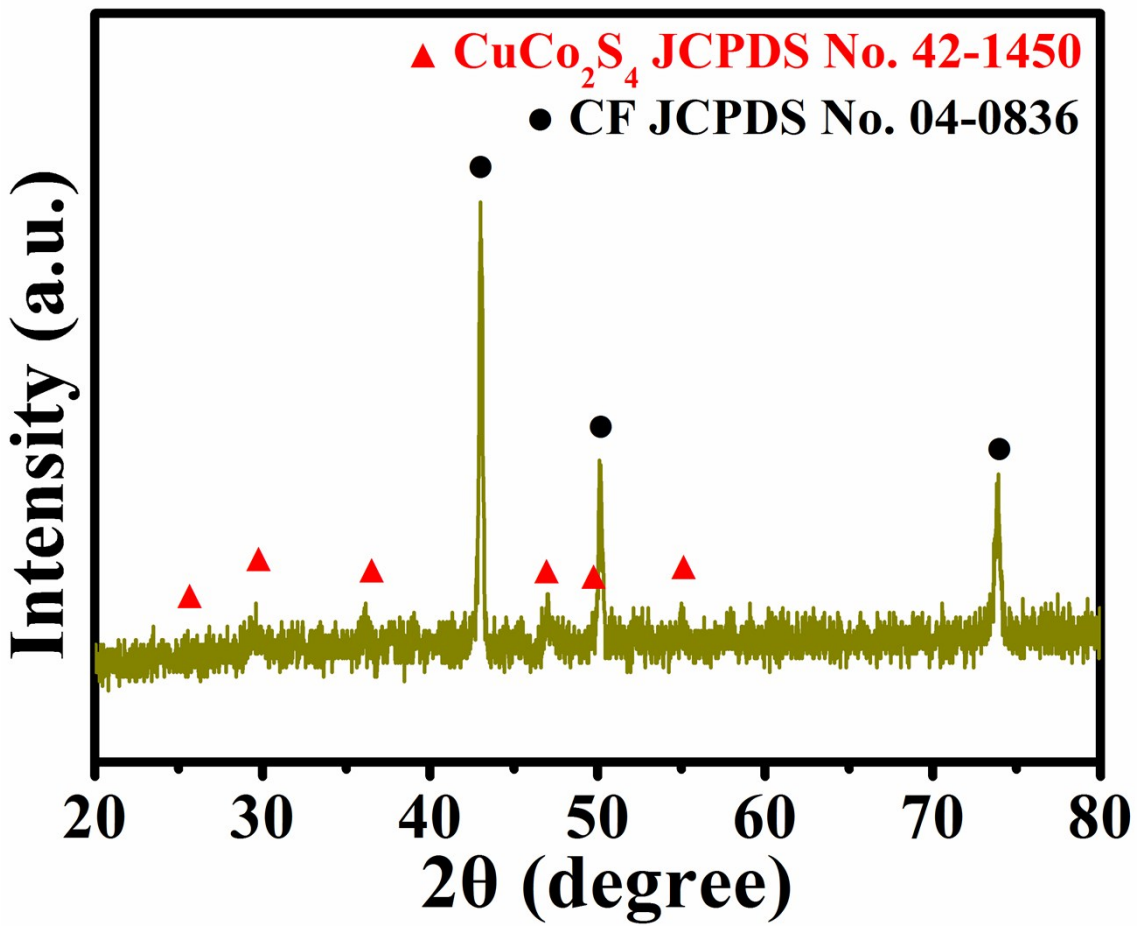

Fig. S9. XRD pattern for $CuCo_2S_4$/CF after water oxidation electrolysis.

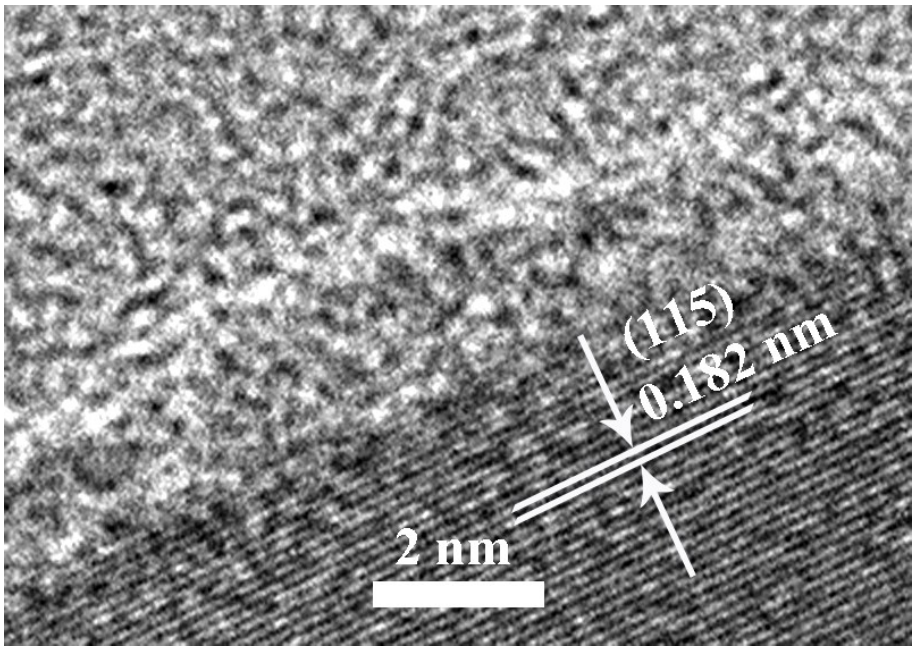

Fig. S10. HRTEM image for $CuCo_2S_4$ after water oxidation electrolysis.

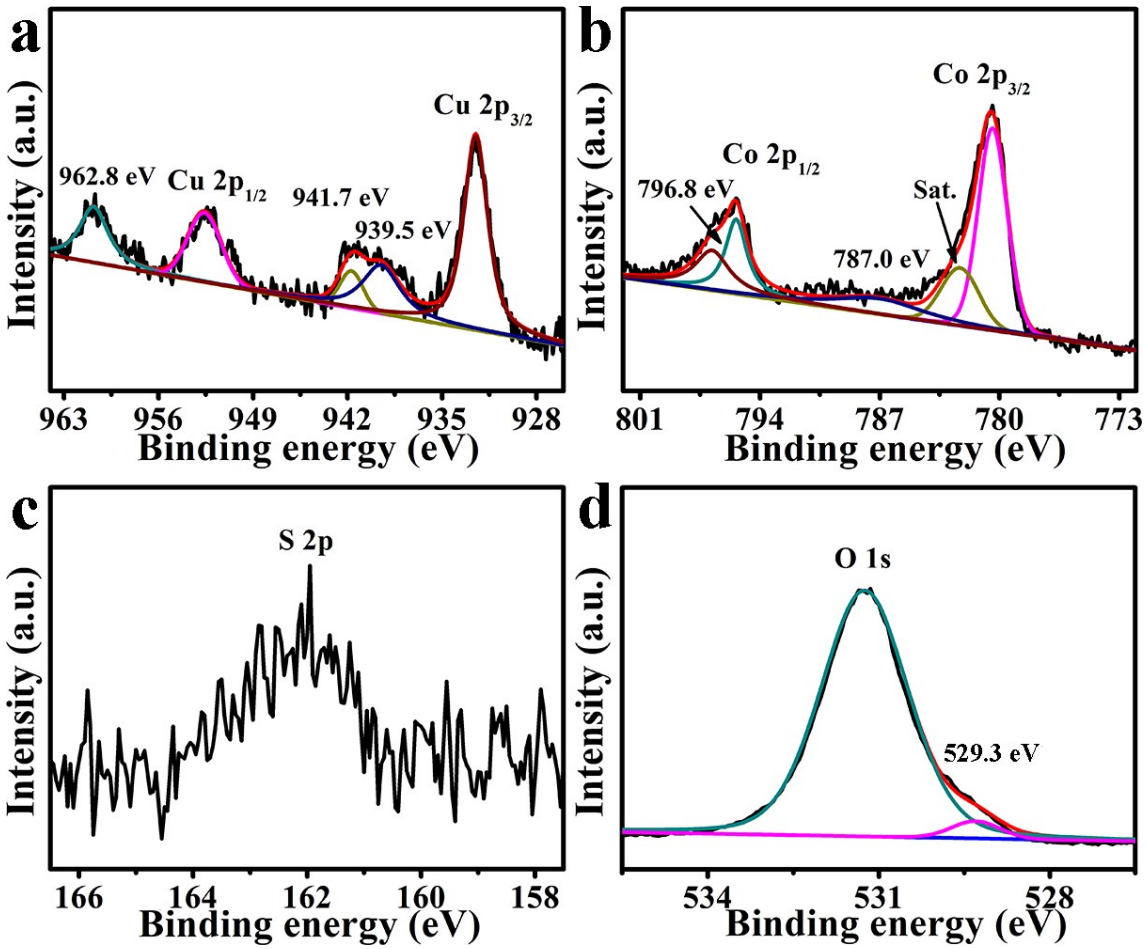

Fig. S11. XPS spectra for $CuCo_2S_4$ in the (a) Cu 2p, (b) Co 2p, (c) S 2p, and (d) O 1s regions after water oxidation electrolysis.

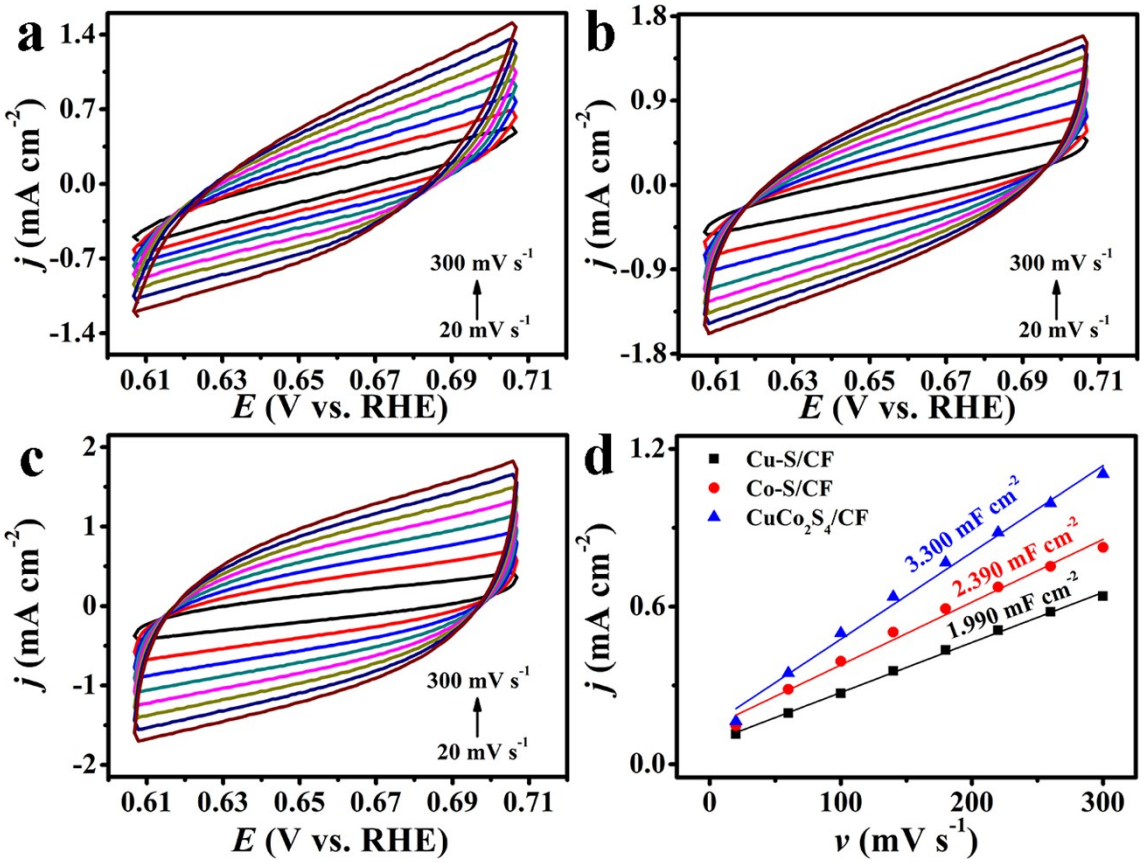

Fig. S12. CVs for (a) Cu–S/CF, (b) Co–S/CF, and (c) $CuCo_2S_4$/CF in the non–faradaic capacitance current range at scan rates of 20, 60 100, 140, 180, 220, 260, and 300 mV s^{-1} in 1.0 M KOH. (d) Corresponding capacitive currents at 0.658 V vs. RHE as a function of scan rate for Cu–S/CF, Co–S/CF, and $CuCo_2S_4$/CF in 1.0 M KOH. The determined double–layer capacitance of the system is taken as the average of the absolute value of the slope for the linear fits to the data.

Table S1. Comparison of water oxidation performance for $CuCo_2S_4$/CF with other non–noble–metal WOCs under alkaline conditions.

Catalyst	j (mA cm^{-2})	η (mV)	Electrolyte	Ref.
$CuCo_2S_4$/CF	60	259	1.0 M KOH	This work
	100	295		
NiFe–LDH/CNT	10	247	1.0 M KOH	3
Cu_3P@NF	10	~320	1.0 M KOH	4
Cu_3P/CF	50	412	0.1 M KOH	5
Mn@$Co_xMn_{3-x}O_4$	10	246	1.0 M KOH	6
NF@NC–$CoFe_2O_4$/C NRAs	10	240	1.0 M KOH	7
NiO@Ni–Bi/CC	10	290	1.0 M KOH	8
benzoate–$Co(OH)_2$/NF	50	291	1.0 M KOH	9
carbonate–$Co(OH)_2$/NF		337		
OCC–8	10	477	0.1 M KOH	10
a–CoSe/Ti	10	292	1.0 M KOH	11
NiMo HNRs/TiM	10	310	1.0 M KOH	12
$MnCo_2S_4$ NA/TM	50	325	1.0 M KOH	13
CoP NA/CC	10	300	1.0 M KOH	14
Co–B@CoO	10	290	1.0 M KOH	15
NiFe–LDH@NiFe–Bi/CC	50	294	1.0 M KOH	16
Fe–NiSe/FeNi foam	100	264	1.0 M KOH	17
NiFe/NF	20	264	1.0 M KOH	18
$Co_{0.13}Ni_{0.87}Se_2$/Ti	100	320	1.0 M KOH	19
$NiCo_2S_4$ NA/CC	100	340	1.0 M KOH	20
NiSe/NF	20	270	1.0 M KOH	21
$NiSe_2$/Ti	20	295	1.0 M KOH	22
Fe–CoP/Ti	10	230	1.0 M KOH	23
Al–CoP/NF	50	280	1.0 M KOH	24
Al–CoP/CC	10	265		
De–LNiFeP/rGO	10	258	1.0 M KOH	25
CeO_2/$CoSe_2$	10	288	0.1 M KOH	26
Co_3O_4/$NiCo_2O_4$	10	340	1.0 M KOH	27
Fe–Co_3O_4	10	486	0.1 M KOH	28
CoO_x@CN	10	260	1.0 M KOH	29
PCPTF film	10	~297	1.0 M KOH	30
$Ni_{2.3\%}$–CoS_2/CC	100	370	1.0 M KOH	31
Ni−Co−S/CF	100	363	1.0 M KOH	32

$Fe_{0.1}$–NiS_2 NA/Ti	100	231	1.0 M KOH	33
$Fe_{11.8\%}$–Ni_3S_2/NF	100	253	1.0 M KOH	34
$NiCo_2S_4$@NiFe LDH/NF	60	201	1.0 M KOH	35
Hollow $Fe_{0.5}V_{0.5}$ spheres	10	390	1.0 M KOH	36
2D CuO nanosheet	10	350	1.0 M KOH	37
$(Co_{0.54}Fe_{0.46})_2P$	10	280	1.0 M KOH	38
FeOOH/CeO_2 HLNTs–NF)	31.3	250	1.0 M NaOH	39
NiFeMn–LDH	10	310	1.0 M KOH	40
nNiFe LDH/NGF	60	~480	0.1 M KOH	41
$Ni_{0.75}V_{0.25}$–LDH	57	350	1.0 M KOH	42
VOOH nanospheres	10	270	1.0 M KOH	43
V/NF	10	292	1.0 M KOH	44
g–C_3N_4/graphene composites	10	539	0.1 M KOH	45
$NiCo_2O_4$@Ni–Co–B/CC	10	270	1.0 M KOH	46
NiCo LDHs	10	367	1.0 M KOH	47
NiCoP NSAs/NF	50	308	1.0 M KOH	48
$CoMoO_4$ micro–flowers	10	312	1.0 M KOH	49
$CoTe_2$ nanofleeces	10	357	0.1 M KOH	50
A–Fe film	10	600	1.0 M NaOH	51
FeB_2	10	296	1.0 M KOH	52
Co_3O_4–MTA	150	360	1.0 M KOH	53
NiCoFe LDH nanoarray	80	257	1.0 M KOH	54
$Zn_xCo_{3-x}O_4$–1:3	10	~320	1.0 M KOH	55

References

1 J. C. Cruz, V. Baglio, S. Siracusano, V. Antonucci, A. S. Aricò, R. Ornelas, L. Ortiz–Frade, G. Osorio–Monreal, S. M. Durón–Torres and L. Arriaga, *Int. J. Electrochem. Sci.,* 2011, **6**, 6607–6619.

2 S. Pintado, S. Goberna–Ferrón, E. C. Escudero–Adán and J. R. Galán–Mascarós, *J. Am. Chem. Soc.*, 2013, **135**, 13270–13273.

3 M. Gong, Y. Li, H. Wang, Y. Liang, J. Wu, J. Zhou, J. Wang, T. Regier, F. Wei and H. Dai, *J. Am. Chem. Soc.*, 2013, **135**, 8452–8455.

4 A. Han, H. Zhang, R. Yuan, H. Ji and P. Du, *ACS Appl. Mater. Interfaces,* 2017, **9**, 2240–2248.

5 C. Hou, Q. Chen, C. Wang, F. Liang, Z. Lin, W. Fu and Y. Chen, *ACS Appl. Mater. Interfaces,* 2016, **8**, 23037–23048.

6 C. Hu, L. Zhang, Z. Zhao, J. Luo, J. Shi, Z. Huang and J. Gong, *Adv. Mater.,* 2017, **29**, 1701820.

7 X. Lu, L. Gu, J. Wang, J. Wu, P. Liao and G. Li, *Adv. Mater.,* 2017, **29**, 1604437.

8 R. Zhang, Z. Wang, S. Hao, R. Ge, X. Ren, F. Qu, G. Du, A. M. Asiri, B. Zheng and X. Sun, *ACS Sustainable Chem. Eng.,* 2017, **5**, 8518–8522.

9 R. Ge, X. Ren, X. Ji, Z. Liu, G. Du, A. M. Asiri, X. Sun and L. Chen, *ChemSusChem,* 2017, **10**, 4004–4008.

10 N. Cheng, Q. Liu, J. Tian, Y. Xue, A. M. Asiri, H. Jiang, Y. He and X. Sun, *Chem. Commun.,* 2015, **51**, 1616–1619.

11 T. Liu, Q. Liu, A. M. Asiri, Y. Luo and X. Sun, *Chem. Commun.,* 2015, **51**, 16683–16686.

12 J. Tian, N. Cheng, Q. Liu, Y. He, X. Sun and A. M. Asiri, *J. Mater. Chem. A,* 2015, 3, 20056–20059.

13 X. Zhang, C. Si, X. Guo, R. Kong and F. Qu, *J. Mater. Chem. A,* 2017, 5, 17211–17215.

14 T. Liu, L. Xie, J. Yang, R. Kong, G. Du, A. M. Asiri, X. Sun and L. Chen, *ChemElectroChem,* 2017, 4, 1840−1845.

15 W. Lu, T. Liu, L. Xie, C. Tang, D. Liu, S. Hao, F. Qu, G. Du, Y. Ma, A. M. Asiri and X. Sun, *Small,* 2017, **13**, 1700805.

16 L. Zhang, R. Zhang, R. Ge, X. Ren, S. Hao, F. Xie, F. Qu, Z. Liu, G. Du, A. M. Asiri, B. Zheng and X. Sun, *Chem. Eur. J.,* 2017, **23**, 11499–11503.

17 C. Tang, A. M. Asiri and X. Sun, *Chem. Commun.,* 2016, **52**, 4529–4532.

18 Q. Luo, M. Peng, X. Sun, Y. Luo and A. M. Asiri, *Int. J. Hydrogen Energy,* 2016, **41**, 8785–8792.

19 T. Liu, A. M. Asiri and X. Sun, *Nanoscale,* 2016, **8**, 3911–3915.

20 D. Liu, Q. Lu, Y. Luo, X. Sun and A. M. Asiri, *Nanoscale,* 2015, **7**, 15122–15126.

21 C. Tang, N. Cheng, Z. Pu, W. Xing and X. Sun, *Angew. Chem., Int. Ed.,* 2015, **54**, 9351–9355.

22 Z. Pu, Y. Luo, A. M. Asiri and X. Sun, *ACS Appl. Mater. Interfaces,* 2016, **8**, 4718–4723.

23 C. Tang, R. Zhang, W. Lu, L. He, X. Jiang, A. M. Asiri and X. Sun, *Adv. Mater.,* 2017, **29**, 1602441.

24 R. Zhang, C. Tang, R. Kong, G. Du, A. M. Asiri, L. Chen and X. Sun, *Nanoscale,* 2017, **9**, 4793–4800.

25 Y. Liu, H. Wang, D. Lin, C. Liu, P. Hsu, W. Liu, W. Chen and Y. Cui, *Energy Environ. Sci.,* 2015, **8**, 1719–1724.

26 Y. Zheng, M. Gao, Q. Gao, H. Li, J. Xu, Z. Wu and S. Yu, *Small,* 2015, **11**, 182–188.

27 H. Hu, B. Guan, B. Xia and X. Lou, *J. Am. Chem. Soc.,* 2015, **137**, 5590–5595.

28 T. Grewe, X. Deng and H. Tüysüz, *Chem. Mater.,* 2014, **26**, 3162–3168.

29 H. Jin, J. Wang, D. Su, Z. Wei, Z. Pang and Y. Wang, *J. Am. Chem. Soc.,* 2015, **137**, 2688–2694.

30 Y. Yang, H. Fei, G. Ruan and J. M. Tour, *Adv. Mater.,* 2015, **27**, 3175–3180.

31 W. Fang, D. Liu, Q. Lu, X. Sun and A. M. Asiri, *Electrochem. Commun.,* 2016, **63**, 60–64.

32 T. Liu, X. Sun, A. M. Asiri and Y. He, *Int. J. Hydrogen Energy,* 2016, **41**, 7264–7269.

33 N. Yang, C. Tang, K. Wang, G. Du, A. M. Asiri and X. Sun, *Nano Res.,* 2016, **9**, 3346–3354.

34 N. Cheng, Q. Liu, A. M. Asiri, W. Xing and X. Sun, *J. Mater. Chem. A,* 2015, **3**, 23207–23212.

35 J. Liu, J. Wang, B. Zhang, Y. Ruan, L. Lv, X. Ji, K. Xu, L. Miao and J. Jiang, *ACS Appl. Mater. Interfaces,* 2017, **9**, 15364–15372.

36 K. Fan, Y. Ji, H. Zou, J. Zhang, B. Zhu, H. Chen, Q. Daniel, Y. Luo, J. Yu and L. Sun, *Angew. Chem., Int. Ed.,* 2017, **56**, 3289–3293.

37 S. M. Pawar, B. S. Pawar, B. Hou, J. Kim, A. T. A. Ahmed, H. S. Chavan, Y. Jo, S. Cho, A. I. Inamdar, J. L. Gunjakar, H. Kim, S. Cha and H. Im, *J. Mater. Chem. A,* 2017, **5**, 12747–12751.

38 A. Mendoza–Garcia, H. Zhu, Y. Yu, Q. Li, L. Zhou, D. Su, M. J. Kramer and S. Sun, *Angew. Chem., Int. Ed.,* 2015, **54**, 9642–9645.

39 J. Feng, S. Ye, H. Xu, Y. Tong and G. Li, *Adv. Mater.,* 2016, **28**, 4698–4703.

40 Z. Lu, L. Qian, Y. Tian, Y. Li, X. Sun and X. Duan, *Chem. Commun.,* 2016, **52**, 908–911.

41 C. Tang, H. Wang, H. Wang, Q. Zhang, G. Tian, J. Nie and F. Wei, *Adv. Mater.,* 2015, **27**, 4516–4522.

42 K. Fan, H. Chen, Y. Ji, H. Huang, P. M. Claesson, Q. Daniel, B. Philippe, H. Rensmo, F. Li, Y. Luo and L. Sun, *Nature Commun.,* 2016, **7**, 11981.

43 H. Shi, H. Liang, F. Ming and Z. Wang, *Angew. Chem.,* 2017, **129**, 588–592.

44 Y. Yu, P. Li, X. Wang, W. Gao, Z. Shen, Y.Zhu, S. Yang, W. Song and K. Ding, *Nanoscale,* 2016, **8**, 10731–10738.

45 J. Tian, Q. Liu, A. M. Asiri, K. A. Alamry and X. Sun, *ChemSusChem,* 2014, **7**, 2125–2130.

46 X. Ji, X. Ren, S. Hao, F. Xie, F. Qu, G. Du, A. M. Asiri and X. Sun, *Inorg. Chem. Front.,* 2017, **4**, 1546–1550.

47 H. Liang, F. Meng, M. Cabán–Acevedo, L. Li, A. Forticaux, L. Xiu, Z. Wang and S. Jin, *Nano Lett.,* 2015, **15**, 1421–1427.

48 Y. Li, H. Zhang, M. Jiang, Y. Kuang, X. Sun and X. Duan, *Nano Res.,* 2016, **9**,

2251–2259.

49 M. Yu, L. Jiang and H. Yang, *Chem. Commun.,* 2015, **51**, 14361–14364.

50 Q. Gao, C. Huang, Y. Ju, M. Gao, J. Liu, D. An, C. Cui, Y. Zheng, W. Li and S. Yu, *Angew. Chem., Int. Ed.,* 2017, **56**, 7769–7773.

51 D. R. Chowdhury, L. Spiccia, S. S. Amritphale, A. Paul and A. Singh, *J. Mater. Chem. A,* 2016, **4**, 3655–3660.

52 H. Li, P. Wen, Q. Li, C. Dun, J. Xing, C. Lu, S. Adhikari, L. Jiang, D. L. Carroll and S. M. Geyer, *Adv. Energy Mater.,* 2017, **7**, 1700513.

53 T. Ma, J. Cao, M. Jaroniec and S. Qiao, *Angew. Chem., Int. Ed.,* 2016, **55**, 1138–1142.

54 Q. Yang, T. Li, Z. Lu, X. Sun and J. Liu, *Nanoscale,* 2014, 6, 11789–11794.

55 X. Liu, Z. Chang, L. Luo, T. Xu, X. Lei, J. Liu and X. Sun, *Chem. Mater.,* 2014, 26, 1889–1895.